Earth Syst. Dynam. Discuss., 6, 1339–1394, 2015
www.earth-syst-dynam-discuss.net/6/1339/2015/
doi:10.5194/esdd-6-1339-2015

Earth System Dynamics
Discussions
Open Access

Groundwater nitrate concentration evolution under climate change and agricultural adaptation scenarios: Prince Edward Island, Canada

D. Paradis[1], H. Vigneault[2], R. Lefebvre[2], M. M. Savard[1], J.-M. Ballard[2], and B. Qian[3]

[1]Natural Resources Canada, Geological Survey of Canada, Quebec City, Canada
[2]Institut national de la recherche scientifique, Centre Eau Terre Environnement (INRS-ETE), Quebec City, Canada
[3]Agriculture and Agri-Food Canada, Eastern Cereal and Oilseed Research Centre, Ottawa, Canada

Received: 17 June 2015 – Accepted: 20 July 2015 – Published: 11 August 2015

Correspondence to: D. Paradis (dparadis@nrcan.gc.ca)

Published by Copernicus Publications on behalf of the European Geosciences Union.

Groundwater nitrate concentration evolution under climate change: Prince Edward Island

D. Paradis et al.

Abstract

Nitrate ($N\text{-}NO_3$) concentration in groundwater, the sole source of potable water in Prince Edward Island (PEI, Canada), currently exceeds the 10 mg L^{-1} ($N\text{-}NO_3$) health threshold for drinking water in 6 % of domestic wells. Increasing climatic and socio-economic pressures on PEI agriculture may further deteriorate groundwater quality. This study assesses how groundwater nitrate concentrations could evolve due to the forecasted climate change and its related potential changes in agricultural practices. For this purpose, a tridimensional numerical groundwater flow and mass transport model was developed for the aquifer system of the entire Island (5660 km^2). A number of different groundwater flow and mass transport simulations were made to evaluate the potential impact of the projected climate change and agricultural adaptation. According to the simulations for year 2050, $N\text{-}NO_3$ concentration would increase due to two main causes: (1) the progressive attainment of steady-state conditions related to present-day nitrogen loadings, and (2) the increase in nitrogen loadings due to changes in agricultural practices provoked by future climatic conditions. The combined effects of equilibration with loadings, climate and agricultural adaptation would lead to a 25 to 32 % increase in $N\text{-}NO_3$ concentration over the Island aquifer system. Climate change alone (practices maintained at their current level) would contribute only 0 to 6 % to that increase according to the various climate scenarios. Moreover, simulated trends in groundwater $N\text{-}NO_3$ concentration suggest that an increased number of domestic wells (more than doubling) would exceed the nitrate drinking water criteria. This study underlines the need to develop and apply better agricultural management practices to ensure sustainability of long-term groundwater resources. The simulations also show that observable benefits from positive changes in agricultural practices would be delayed in time due to the slow dynamics of nitrate transport within the aquifer system.

ESDD
6, 1339–1394, 2015

1 Introduction

Significant increases in nitrate content of groundwater are caused largely by sewage leaks, wastewater treatment without denitrification, improper management of wastewater effluents and overuse of fertilizers and/or animal waste. These nitrate sources are responsible for the contamination of numerous aquifers, especially in those areas where groundwater is replenished directly from the surface over large areas. Nitrate contamination is often associated with anthropogenic activities at ground surface, such as the fertilization of agricultural crops. Once groundwater is contaminated, remediation is difficult, thus the prevention of contamination is the primary strategy used for water quality management (Ghiglieri et al., 2009).

Groundwater is the sole source of potable water in the Province of Prince Edward Island (PEI) in eastern Canada, and it plays a dominant role in surface water quality as well. Besides being a concern for drinking water quality, excessive nitrate levels contribute to eutrophication of surface waters, especially in estuarine environments (Somers and Mutch, 1999). Only one watershed among the 50 watersheds delineated in PEI still has a mean nitrate concentration in groundwater within natural background levels ($< 1\,\mathrm{mg\,L^{-1}}$ N-NO_3). Furthermore 6 % of supply wells exceed the recommended maximum concentration limit of $10\,\mathrm{mg\,L^{-1}}$ (N-NO_3) for drinking water (Health Canada, 2014; Somers, 1998; Somers et al., 1999). Over the past decade, several studies have documented the nitrate problem in PEI groundwater (Somers, 1998; Somers et al., 1999; Young et al., 2002; Savard et al., 2007) and suggested that elevated nitrate levels are often associated with agricultural activities, especially the use of fertilizers for row crop production. In addition, water quality surveys have recorded important increases (more than doubling since 1980) of nitrate concentrations in ground and surface waters in some areas of the province (Somers et al., 1999).

According to simulations made with the Global Circulation Model (GCM) for Canada, temperature increases in the order of 2 to 4 °C by 2050 is expected at the country scale (Hengeveld, 2000). Projected changes in annual precipitation over Canada re-

ESDD
6, 1339–1394, 2015
Groundwater nitrate concentration evolution under climate change: Prince Edward Island
D. Paradis et al.

main within 10 % of present levels until 2050, with most of the increases occurring during winter months. Since global warming is expected to change the hydrologic cycle (Gleick, 1986) as well as the agricultural practices (Olesen and Bindi, 2002; McGinn and Shepherd, 2003), it could, in turn, impact groundwater nitrate concentrations. The overall impact on groundwater nitrate will likely depend on both the magnitude of the change induced by climate change on the hydrologic cycle and how agriculture will adapt to these changes. The combined pressures of climatic change on groundwater recharge and agricultural practices, together with the need to preserve groundwater quality for the residents of PEI illustrate the importance of effective long-term strategies for water management. The aim of this study is then to assess the potential impact of both climate change and modified agricultural practices on future groundwater nitrate concentrations for the entire PEI ($\sim 5660\,km^2$).

Nitrate concentrations in groundwater depend on the mass loadings and the amount of water infiltrating the soils down to the water table. In other words, future $N\text{-}NO_3$ concentration can be estimated as the mass of nitrate leached over the volume of recharge per unit area carrying out this mass to the aquifer (groundwater recharge) under projected climatic conditions. Climate change impacts were simulated using different global circulation models (GCMs) and CO_2 emission scenarios for the period of 2040–2069, to assess the sensitivity of the climatic variables. The stochastic weather generator AAFC-WG (Hayhoe, 2000) was then used to adjust daily temperature and precipitation of selected large-scale CGM scenarios to the scale of the Island and allow simulations of groundwater recharge over the Island using the hydrologic infiltration model HELP (Schroeder et al., 1994). The physical parameters used by this infiltration model allow an assessment of the impact of changing climatic parameters on the hydrological cycle, which includes groundwater recharge. Moreover, the amount of nitrogen leaching to the aquifer was estimated on the basis of the residual soil nitrogen (RSN) indicator (Yang et al., 2007) under present-day conditions as well as considering agricultural adaptation scenarios in response to the increase of crop heat units, effective growing degree-days and agro-economic trends (De Jong et al., 2008).

ESDD
6, 1339–1394, 2015

Studying the impacts of climate change and agricultural management scenarios on groundwater quality also necessitates understanding the aquifer system dynamics. Particularly, flow and transport simulations are needed to assess the nitrate residence time and the aquifer response to changes in practices or climatic conditions. While there have been many studies relating the effect of climate changes on groundwater resources (e.g. Yussof et al., 2002; Allen et al., 2004; Scibek and Allen, 2006; Green et al., 2007a, b; Hsu et al., 2007; Jyrkama and Sykes, 2007; Serrat-Capdevila et al., 2007; Woldeamlak et al., 2007; Holman et al., 2009; Allen et al., 2010; Crosbie et al., 2010; McCallum et al., 2010; Okkonen et al., 2010; Rozell and Wong, 2010; Zhou et al., 2010; Beigi and Tsai, 2015), there are few published studies which attempt to relate climate change to changes in nitrate concentrations in groundwater (e.g. De Jong et al., 2008; Ducharne et al., 2007; Holman et al., 2005a, b; Jackson et al., 2007). In their works, De Jong et al. (2008) and Jackson et al. (2007) estimated mass of nitrogen leaching through the unsaturated zone for different scenarios to relate with nitrate concentrations measured in wells. That is, assuming a direct relationship between nitrate leachate and groundwater nitrate concentrations regardless of the aquifer system dynamics. While the semi-empirical hydrological model proposed by Holman et al. (2005a, b) to predict nitrate concentrations in both surface water and groundwater includes a groundwater store, such model does not simulate spatial and temporal groundwater flow patterns that control nitrate transport in the aquifer system. For instance, Ducharne et al. (2007) demonstrated that modeling of the aquifer system using a physically based groundwater flow model allowed to simulate the inertia of the aquifer system, which has a considerable impact on nitrate concentrations measured in wells. In this study, the evolution of groundwater nitrate concentrations under a changing climate was modeled using the physically-based groundwater flow and solute transport numerical simulator FEFLOW (Finite Element subsurface FLOW system; Diersch, 2010) considering the effect of the dual porosity of the fractured porous medium (sandstone), identified by Jackson et al. (1990) as being responsible for the persistence of pesticides in the aquifer system of PEI. In particular, the hydrogeolog-

ESDD
6, 1339–1394, 2015

ical model developed for the entire Province was based on knowledge gained from the Wilmot watershed (Jiang and Somers, 2009; Paradis et al., 2006, 2007), which is representative of most other regions of PEI regarding land use, soils, physiography, geology and hydrogeology. The hydrogeological model was calibrated with historical hydrogeological records of conditions specific to the Island: hydraulic heads, groundwater discharge to river and nitrate concentrations measured in both wells and rivers.

The novelty of this study is to provide a quantitative comparison of climate change effects and agricultural adaptation impacts on the future evolution of nitrate concentration, taking into account potential changes in groundwater recharge and nitrate loadings. Also, the general framework developed for the integration of the knowledge related to the aquifer system, climatic parameters and agricultural practices into a comprehensive numerical model calibrated with site-specific records could be applied elsewhere to guide groundwater resource and quality management.

2 Prince Edward Island study area

PEI, located in eastern Canada, covers approximately 5660 km^2 and is 225 km long by 3 to 65 km wide (Fig. 1 and Table 1). Topographic elevation ranges from sea level to 140 m a.s.l. PEI is predominantly rural, with 39 % of its surface covered by agricultural lands and 45 % by forests. Forests mostly cover the eastern and western portions of the Island, whereas agricultural activities are mostly concentrated in the central part. Residential, urban and industrial activities occupy less than 6 % of the territory.

2.1 Climate and hydrology

The climate in the Island is humid continental, with long, fairly cold, winters and warm summers. Data selected from four weather stations geographically distributed across the Island (Fig. 1) show relatively similar conditions (Table 2). As an example of the climatic conditions found on the Island, the mean annual precipitation at the Charlotte-

ESDD
6, 1339–1394, 2015

town weather station is 1173 mm, most of which falls as rain (75 %). The mean annual temperature is about 5.3 °C and means for monthly temperature range from −8 °C in January to 18.5 °C in July. The Island can be divided into fifty (50) watersheds comprising 241 sub-watersheds (Fig. 1). River basins are typically small, and the main rivers are estuarial over a significant portion of their length. Mean annual streamflow ranges from less than 0.66 to 2.88 $m^3 s^{-1}$ (Table 3).

2.2 Geology and hydrogeological framework

PEI is a crescent-shaped cuesta of continental red beds, Upper Pennsylvanian to Middle Permian in age, dipping to the northeast at about one to three degrees (Van de Poll, 1983). Van de Poll (1983) mapped the red bed units as an upward-fining series of cyclic deposits containing four megacycles. These sequences consist of conglomerate, sandstone and siltstone red beds, in which sandstones are dominant. These units exhibit rapid lateral and vertical facies changes and strong cross-bedding features. The rock sequence underlying the Island is almost entirely covered by a layer of unconsolidated glacial material from a few centimetres to several meters in thickness (Prest, 1973). These deposits are generally derived from local sedimentary rock and include both unsorted tills and water-worked glacio-fluvial and glacio-marine deposits.

With few exceptions, the surficial sediments over PEI do not represent significant aquifers as they are not water saturated, so the sandstone constitutes the main aquifer. Because the geology of the Island is relatively homogeneous, the hydrogeological conceptual model for all PEI is assumed to be similar to the one defined for the Winter River and Wilmot River watersheds where Francis (1989) and Paradis et al. (2006, 2007) carried out extensive hydrogeological characterization. Based on these studies several observations relative to the hydrogeological framework of PEI can be made:

- The sandstone aquifer comprises a shallow high-flow system overlying a deep low-flow system (Fig. 2a). This is based on hydraulic conductivity profiles obtained from field multi-level packer tests in rock aquifer wells that show a rapid decrease

ESDD
6, 1339–1394, 2015

of hydraulic conductivity with depth (Fig. 2b). This decrease is significant under a depth of 18 to 36 m, according to location. The shallow interval with higher permeability is defined as the high-flow system. Most domestic wells tap potable water in this high-flow system (Mutch, 1998; Rivard et al., 2008).

- The sandstone aquifer represents a double porosity system with fractures providing groundwater flow paths and the porous matrix providing storage capacity, both for water and solutes, including nitrate. The fractured sandstone is characterized by relatively high hydraulic conductivity, between 1×10^{-6} and 3×10^{-4} m s^{-1} (Fig. 3b), but it has a low storage capacity (1–3 %), as obtained from modelling of baseflow recession curves (Paradis et al., 2006, 2007) and seasonal nitrate sources in groundwater from isotopes (Ballard et al., 2009). In contrast, the matrix has a high porosity of about 17 %, but a much lower hydraulic conductivity as measured from laboratory core permeameter tests: mostly between 1×10^{-8} and 5×10^{-7} m s^{-1} but as low as 5×10^{-10} m s^{-1} for mudstone (Francis, 1989).

- Comparison between field (Paradis et al., 2006, 2007; Francis, 1989) and laboratory (Francis, 1989) hydraulic conductivity measurements suggests that fractures play an important role in the rock aquifer permeability, and the general decrease in hydraulic conductivity with depth is the result of decreasing fracture aperture and frequency. Horizontal bedding of the sandstone forms the main fracture network above 35 m depth (82 % of all fractures; Francis, 1989). Over a large area, the relative homogeneity of the distribution and interconnection of fractures provides a typical "porous media" response to pumping, especially in the weathered high-flow rock aquifer system (Francis, 1989).

- Tritium analyses on groundwater samples in the high-flow system indicate the presence of "modern groundwater" younger than 50 years. In the low-flow system, no tritium is observed but Carbon-14 analyses provide groundwater ages between 5000 and 7000 years at depths ranging between 50 and 85 m below the water table (Paradis et al., 2006, 2007).

ESDD
6, 1339–1394, 2015

– Transient modelling of baseflow recession curves (the groundwater contribution to a river) for the Wilmot River watershed suggests that rivers gain water from the aquifer most of the year (Jiang and Somers, 2009) and there is a strong interaction between the high-flow system and the rivers (Paradis et al., 2007). This is also supported by seasonal sampling of nitrate carried out over a period of two years in domestic wells and in the Wilmot River that shows similar average nitrate concentrations as well as water and nitrate isotope properties (Savard et al., 2007, 2010).

In summary, it is inferred from the development of the conceptual hydrogeological model that groundwater flow and nitrate transport predominantly occur in the high-flow system. The shallow high-flow system essentially follows the ground topography and is hydraulically connected to rivers. Nitrate transported to the aquifer by infiltration of precipitation will first reach the shallow high-flow system and then eventually reach rivers mainly through fractures in weathered and fractured sandstone, which are fairly more permeable than the sandstone matrix itself. Nitrate transport rate through the aquifer system could however be reduced as matrix diffusion occurs due to the contrast in nitrate concentration between fractures and matrices. The high porosity of the sandstone matrix makes it an important repository for nitrate which could store or release nitrate, depending on geochemical conditions in the adjacent fracture network. Finally, it is also likely that a proportion of the nitrate transported in the high-flow system has also reached the underlying low-flow system. Considering the reduced groundwater flow and the mostly old groundwater ages encountered in the low-flow system, the nitrate that may be present in the low-flow system may not have reached rivers yet. Note that in the case of the entire PEI, oxidizing aquifer conditions usually prevail in the sandstone aquifer and it was assumed that denitrification processes are negligible within the aquifer. Moreover, no natural geological sources of nitrate are expected to be present throughout the Island. The aquifer nitrate concentrations would then be controlled by water infiltration and nitrate leaching from the soil.

ESDD
6, 1339–1394, 2015

3 Study methodology

Figure 3 presents the general workflow followed in this study to model the evolution of nitrate concentrations in groundwater of the PEI aquifer system under a changing climate, which is briefly described below with further details provided in the following sections:

- Climate change can itself be predicted on the basis of meteorological models with a large degree of uncertainty. Therefore, different climate change scenarios have to be considered in order to represent the potential range of impacts, especially those related to predicted temperature and precipitation. To assess the impact of climate change and agricultural adaptation on groundwater nitrate concentrations, four climate scenarios were selected to provide future daily weather conditions for the period 2040–2069. These climate scenarios are based on different global circulation models (GCMs) and CO_2 emission scenarios for the period 2040–2069.

- The daily temperatures and precipitations of selected large-scale CGMs for the four climate scenarios were downscaled using historical meteorological records of existing weather stations using the stochastic weather generator AAFC-WG (Hayhoe, 2000) in order to provide more realistic climate conditions of the Island.

- Nitrogen leaching to the aquifer was estimated under present-day conditions and agricultural adaptation scenarios. These nitrate loadings are determined on the basis of the residual soil nitrogen (RSN) indicator (Yang et al., 2007).

- Groundwater recharge was obtained from the HELP infiltration model (Schroeder, 1994), which uses daily climate conditions and soil properties as input. As done by Croteau et al. (2010), recharge obtained from HELP was calibrated on the basis of present-day climate conditions, so that future recharge could be estimated using the four climate scenarios.

ESDD
6, 1339–1394, 2015

- Using present-day nitrate loadings and groundwater recharge, a three-dimensional numerical model of groundwater flow and nitrate transport was developed and calibrated for the entire PEI using FEFLOW (Diersch, 2004) in order to represent the specific hydrogeological conditions of the Island. This model was then used to simulate the future evolution of nitrate concentrations under different climate change and agricultural adaptation scenarios that implied potential changes in groundwater recharge and nitrate loadings.

3.1 Climate change scenarios and climate data downscaling

In this study, daily climate data are used as inputs to simulate groundwater recharge and nitrogen leaching under historical as well as potential climate change scenarios (Fig. 3). For the study area, coupled atmosphere and ocean general circulation models are currently the most reliable tools available for projecting future climate changes. However, resolutions of these models are coarse and downscaling is necessary to predict realistic climate characteristics at the local scale. Because the impact model needs continuous climatic record without missing values, the AAFC-WG (Hayhoe, 2000) was used to generate synthetic continuous daily weather records for the historical period (1971–2000) and for two (2040–2069) climate scenarios using different GCMs (Fig. 3). The AAFC-WG is a stochastic weather generator that uses transition probabilities (2-state Markov chain) for determining the status (wet or dry day) and empirical distribution of precipitation and estimating both, precipitation amounts on wet day and daily temperature (minimum and maximum). This stochastic weather generator was developed for and evaluated in diverse Canadian climates (Qian et al., 2004).

The Intergovernmental Panel on Climate Change Special Report on Emission Scenarios (Nakicenovic and Swart, 2000) provides 40 different scenarios, which are all deemed “equally likely”, but the A2 and B2 scenarios are widely adopted in climate change experiments and impact studies (IPCC, 2001). The A2 scenario envisions a population growth to 15 billion by year 2100 with rather slow economic growth and development. Consequently, the projected equivalent CO_2 concentration rises from

ESDD
6, 1339–1394, 2015

476 ppm in 1990 to 1320 ppm in 2100. The B2 scenario envisions slower population growth (10.4 billion by 2100) with a more rapidly evolving economy, but with more emphasis on environmental protection. It therefore produces lower emissions (CO_2 concentration of 915 ppm by 2100) and less warming than scenario A2. The A2 and B2 scenarios were simulated using two different GCMs, which are the CGCM2 (Flato and Boer, 2001) developed at the Canadian Centre for Climate Modelling and Analysis, and HadCM3 (Gordon et al., 2000) developed at the Hadley Centre for Climate Prediction and Research of the UK Meteorological Office. Daily outputs of maximum and minimum air temperature, and total precipitation were obtained electronically from the Canadian Centre for Climate Modelling and Analysis and the Hadley Centre through the Climate Impacts LINK project (Viner, 1996) for the four climate change scenarios labelled hereafter: CGCM2-A2, CGCM2-B2, HadCM3-A2 and HadCM3-B2.

To obtain future climate data, daily outputs from the four climate change scenarios were downscaled using the AAFC-WG with observed historical climate data from existing weather stations. A total of eleven weather stations were selected, covering PEI fairly evenly and having the best available historical weather data for 1971–2000 (Fig. 1). Observed historical weather data, including daily maximum and minimum air temperatures and daily precipitation, were provided by Environment Canada through their web site, and first used to calibrate an AAFC-WG model for each weather station. The parameters for the various statistical models used by the AAFC-WG were indeed estimated from historical observations independently for each station. The following steps were then followed for each climate scenario (CGCM2-A2, CGCM2-B2, HadCM3-A2 and HadCM3-B2) to generate future downscaled climate data (Qiang and De Jong, 2007):

- statistics are computed for daily precipitation and temperature (minimum and maximum) for each of the four closest GCM grid nodes surrounding each weather station for both the synthetic historical (1971–2000) and future (2040–2069) periods;

Discussion Paper | Discussion Paper | Discussion Paper | Discussion Paper |

ESDD

6, 1339–1394, 2015

Groundwater nitrate concentration evolution under climate change: Prince Edward Island

D. Paradis et al.

Title Page
Abstract Introduction
Conclusions References
Tables Figures
◀ ▶
Back Close
Full Screen / Esc
Printer-friendly Version
Interactive Discussion

- changes in statistics between the synthetic historical and future period are calculated either as ratios (precipitation-related variables) or as differences (temperature-related variables);
- the ratios and differences are interpolated from the GCM grid nodes to each weather station location using the nearest neighbour approach, weighing each neighbour by the inverse squared distance;
- interpolated ratios and differences are applied to perturb the statistical parameters of each calibrated AAFC-WG model with observed historical data to form a new set of model parameters for the future period; and
- ten stochastic 30 year long daily climate synthetic series for the 2040–2069 period are generated using the new set of model parameters for each station.

Note that in this study, daily synthetic climate data corresponds to the average of the ten stochastic simulations.

3.2 Groundwater recharge

Groundwater recharge simulations serving as input for the FEFLOW hydrogeological model (see discussion below) was carried out with the physically based hydrologic model HELP (Schroeder et al., 1994) (Fig. 3). This model was initially developed for predicting landfill hydrologic processes, testing the effectiveness of landfill designs, and predicting landfill design feasibility, but HELP has also been used to estimate groundwater recharge (e.g. Jyrkama et al., 2002; Allen et al., 2004; Croteau et al., 2010; Rivard et al., 2014). The model is quasi two-dimensional and requires input for weather (precipitation, solar radiation, temperature, and evapotranspiration), soil (porosity, field capacity, wilting point, and hydraulic conductivity), and engineering design data (liners, leachate and runoff collection systems, and surface slope). HELP uses numerical-solution techniques that account for the effects of surface storage, snowmelt, runoff, infiltration, evapotranspiration, vegetative growth, soil moisture storage, and various

ESDD
6, 1339–1394, 2015

engineering parameters (e.g. lateral subsurface drainage). The natural water balance components that the program simulates include precipitation, interception of rainwater by leaves, evaporation by leaves, surface runoff, evaporation from soil, plant transpiration, snow accumulation and melting, and percolation of water through the soil profile. The advantage of using such a model is that temperature and precipitation resulting from climate scenarios may be directly used in the model to predict future groundwater recharge rate, once the model has been calibrated based on present-day data.

The spatial estimation of groundwater recharge over PEI was obtained using 500 m × 500 m cells (total of 21 168). For each cell, model parameters were retrieved and analyzed with geographical information software and a database management system. The HELP parameters used are summarized below.

- Soil profile: the soil profile is the vertical combination of natural soil and geological materials that compose the vadose and saturated zones. The surface soil information was assembled from various regional soil surveys conducted on the Island (Canadian Soil Information System, 2000). There were a total of 953 unique soil types identified on PEI that were regrouped into 6 distinct soil classes. A typical soil profile consisting of three layers was used to their representation. The top layer is 0.5 m thick and consists of one of the 6-soil class; layer 2 is 1–17 m thick and consists of unconsolidated glacial material; and bottom layer is 10 m thick and consists of weathered sandstone (high-flow system).

- Initial moisture content: the initial water content of each soil profile layers was computed by the model as steady state values. HELP indeed assigned values for the initial water moisture storage of layers and simulates a one-year period. These values were then used as initial values for the simulations. A sensitivity analysis of initial water content reveals that this parameter does not affect significantly groundwater recharge estimates as steady state conditions can be assumed over the long simulation period.

ESDD
6, 1339–1394, 2015

– Surface runoff: surface runoff (also known as overland flow) is the flow of water that occurs when excess rainfall or snowmelt flows over the soil surface. Surface runoff was estimated using modified Soil Conservation Service (SCS) curve-number method (USDA, 1986), as proposed by Monfet (1979). The modified method allows a more reliable estimation of surface runoff in watersheds with short concentration time and for precipitation patterns found in eastern Canada. The modified SCS method allows estimation of surface runoff to a river following a rainfall or snowmelt event using soil characteristics, land use, type of vegetation, soil humidity, and surface slope. Digital land use and land cover data were obtained from Landsat-7 images (CanImage, 2001).

– Solar radiation: the required daily values of precipitation, mean air temperature, and solar radiation were calculated. Precipitation and temperature were obtained from downscaled climate scenarios, while solar radiation data were generated using the weather generator provided by HELP. Solar radiation is computed according to precipitation (whether the day is wet or dry) and latitude.

– Evapotranspiration: the multi-layer procedure for calculating evaporation values from snow, soil, and leaves, as well as transpiration based on type of vegetation used the evaporative zone depth, maximum leaf-area index, growing season start and end day, average wind speed, and relative humidity. These parameters were evaluated from existing land cover, agricultural and climatic data.

Groundwater recharge values simulated from the model were calibrated against baseflow values estimated using the method of hydrograph separation with streamflow records (Furey and Gupta, 2001). This approach was selected because of the general uncertainty in several of the input parameters of HELP (e.g. Croteau et al., 2010). Baseflow is the groundwater contribution to river discharge (streamflow) and it is often used as an approximation of groundwater recharge when underflow (groundwater flow beneath and by-passing a river), evapotranspiration from riparian vegetation, and other losses of groundwater from the watershed are minimal (Risser et al., 2005). Hy-

ESDD
6, 1339–1394, 2015

drograph separation methods estimate the part of the streamflow hydrograph attributed to baseflow using semi-empirical filter techniques.

The HELP model was then run with the historical records of temperature and precipitation (1971–2000) and annual groundwater recharge values were calibrated against baseflow estimated using hydrograph separation method for three gauged streamflow stations with the most comprehensive time series (Fig. 4; Morell, Wilmot and Winter, Fig. 1 for location). For each watershed, groundwater recharge with HELP was estimated by summing all individual 1-D soil profiles included in the watershed assuming that water reaching the aquifer for each soil profile contributes to the streamflow within the year. The most relevant parameters to calibrate were the evaporative zone depth, the initial soil moisture conditions, and the heat insulation of the snow cover. In particular, it was observed from analysis of well hydrographs that groundwater recharge can occur throughout the year, including winter. Winter recharge is due to the heat insulation effect of the snow cover, and thawing, when air temperature is above 0 °C, combined with heavy rainfall. To reproduce the winter groundwater recharge, which can account for up to 20 % of the annual recharge, the original HELP code was modified to consider the heat insulation effect of the snow cover. A simple analytical calculation based on air temperature, and typical snow cover thickness and density for the PEI showed indeed that air temperature must be below −3 °C to freeze the ground at the soil–snow interface to create a barrier to water infiltration. Then the HELP code was modified to start freezing the ground at −3 °C to allow winter recharge. Groundwater recharge estimated with HELP are comparable to baseflow estimated with the Furey and Gupta (2001) method (Fig. 4), with a correlation coefficient of 64 %. Results of the calibration show also that seasonal (winter, spring, summer, fall) groundwater recharge values are within 4 to 17 % on average.

ESDD
6, 1339–1394, 2015

3.3 Mass of nitrogen available for leaching and agricultural adaptation scenarios

The nitrogen mass available for transfer to groundwater was estimated with the residual soil nitrogen (RSN) indicator (Drury et al., 2007; Fig. 3). The RSN indicator estimates the quantity of inorganic soil nitrogen at the time of harvest, at the Soil Landscape of Canada (SLC) polygon level (Soil Landscapes of Canada Working Group, 2006). The RSN indicator is the difference between nitrogen inputs from chemical fertilizers, manure, biological nitrogen fixation, and atmospheric deposition and outputs in the form of nitrogen in the harvested portion of the crops and gaseous losses to the atmosphere. Although soil mineralization and immobilization also occur on a seasonal basis, it is assumed that soils are in a steady state situation, with no net change in soil organic nitrogen from one year to the next.

Nitrogen losses during manure storage, and therefore the amount of available nitrogen for land application, vary with manure source, storage methods and manure form (liquid, solid, compost). It is estimated that 15 % of manure nitrogen is lost during storage and handling (Burton and Beauchamp, 1986), 35 % is added to the soil as organic nitrogen (Ontario Ministry of Agriculture and Food, 2003), and consequently 50 % of nitrogen originally present in manure is inorganic nitrogen which would be available to crops during the year of application. Of this available nitrogen, 1.25 % is lost as nitrous oxide emissions, and an equal portion is assumed to be lost through N_2 production.

The main inputs of the RSN model consist of acreages for all major agricultural crops and their associated crop yields, as well as the type and number of livestock. These data are collected every five years through the census made by Agriculture and Agri-Food Canada and are allocated to SLC polygons based on the methodology described by Huffman et al. (2006). The RSN model was run for all five-census years (1981, 1986, 1991, 1996 and 2001) and the output was averaged to obtain a “historical” RSN value for each of the 23 SLC polygons covering PEI (details in De Jong et al., 2008).

ESDD
6, 1339–1394, 2015

Many different agricultural adaptation scenarios can be devised, either with increased or decreased production intensity as compared to the present level. For the purpose of our study, a "worst case" scenario was selected because none of the adaptation scenarios is verifiable. Based on consensus expert opinion of Agriculture and Agri-Food Canada at the Research and Policy Branch, it was assumed that agricultural production in PEI would intensify over the next 50 years. Hence, relative to the 2001 census provincial totals, the following sequential agricultural land use scenario was developed for the 2040–2069 period (De Jong et al., 2008):

- the area of alfalfa, improved pasture, tame hay and other grain cereals reduces by 40, 30, 30 and 15 %, respectively (total "freed-up" area: 29 794 ha);
- the berries and vegetable area increases by 100 % (remaining "freed-up" area: 25 179 ha);
- Of the remaining "freed-up" area, 20, 40 and 40 % is allocated to potatoes, grain corn and soybeans, respectively;
- buffer strips, a legislative requirement, reduce the increased total area of potatoes by 5 %, with this area going into the "other land" category;
- for SLCs 538 001, 537 002 and 537 003, the total area of potatoes decreases by 6 %, because these SLCs contain fields with steep slopes, and the "freed-up" area is allocated equally to tame hay and spring wheat;
- as a consequence of the decrease in perennial forages, the number of cattle decreases by 10 %; and
- the number of poultry and pigs increases by 30 %.

In order to calculate RSN for this agricultural adaptation scenario, data on nitrogen fertilizer recommendations and estimated crop yields were needed. Based on CGCM1-A scenarios for the years 2040–2069, Bootsma et al. (2001) report that crop heat units

ESDD
6, 1339–1394, 2015

should increase to 3000–3200 in PEI and effective growing degree-days will increase to 1800–2000. For this study the 1996 crop yields of Ontario (2001 was a drought year) were used for the PEI climate change scenario 2040–2069 because the current crop heat units and effective growing degree-days are similar to those in Ontario. To properly balance future crop nitrogen demands with fertilizer nitrogen supplies, we also used the Ontario nitrogen fertilization recommendations for the PEI climate change scenario. As done by De Jong et al. (2008), the model was then run with this scenario to obtain 23 projected RSN values one for each polygon for the four climate scenarios.

The nitrogen load was applied on the SLC polygons because RSN values are estimated over these entire polygons. RSN units are provided in kg of nitrogen per hectare of farmland area but farmlands are not defined within the SLC polygon. Hence, to be compatible with the hydrogeological model (see description below), the nitrogen load applied at the surface of the model was estimated by multiplying the RSN values by the ratio of farmland area over SLC polygon area. This operation maintains the total nitrogen mass over the SLC polygon but reduces the applied rate. For modelling purposes, it was assumed that the total RSN was nitrified and leached to the aquifer within the year, which provides conservative scenarios.

3.4 Numerical groundwater flow and nitrate transport model

To represent the groundwater flow system and to simulate nitrate transport under the historical and various climate scenarios, the FEFLOW numerical model was divided into eight layers (Fig. 5), four sheets to represent the shallow high-flow system, and four, for the deep low-flow system. The base of the model is deep at approximately 800 m below water table to include the different flow patterns that can develop within the PEI aquifer system (e.g. Tóth, 1963). The vadose zone was not represented in the model because water-table level fluctuations resulting from infiltrated precipitation generally show short lag-time response of only a few days. However, the upper nodes of the first layer were allowed to move with water table fluctuations in order to better estimate water and nitrate fluxes in the high-flow system. Boundary conditions include

ESDD
6, 1339–1394, 2015

constant heads around the Island in the first layer, and no flow boundaries in the underlying layers to simulate the flow along the saline front around the Island (Fig. 5). Constant heads were also applied to rivers on the first layer to represent the hydraulic connection between rivers and the high-flow system. The resulting three-dimensional grid contains 4 896 246 6-node prismatic triangular elements with an average element area of 0.0925 km^2 (with triangle edges of approximately 430 m).

The PEI groundwater flow and nitrate transport model was calibrated with three different types of data: (1) hydraulic heads measured in domestic wells, (2) baseflow-recession curves for the main rivers and, (3) groundwater nitrate concentrations recorded in domestic wells. While independent data sets were used to calibrate the FEFLOW model, the calibration process followed a sequential procedure, as summarized in the next sub-sections. Note that non-pumping conditions were considered for the calibration and future scenarios, as most of the Island is supplied by individual domestic wells sparsely spread over the Island (approximately 145 000 inhabitants in 2014, over 5660 km^2). The impact of pumping wells on the water table is thus expected to be low ($< 2\,mm\,yr^{-1}$ based on a daily individual consumption of 200 L), except in few localized areas where potable water is supplied by production wells (e.g. Charlottetown). Irrigation water for agriculture and associated return flow were not considered either because rainfall generally supplies the needed water demand for crops irrigation.

3.4.1 Hydraulic heads calibration

The calibration of the FEFLOW model was first carried out under steady-state conditions with hydraulic head values measured at the time of drilling in more than 700 wells (Fig. 6a). These wells are domestic water wells, of varying depth, which generally end in the shallow high-flow system. Hydraulic heads were used to adjust the hydraulic conductivity within reported the range of values while keeping calibrated groundwater recharge values from the HELP model unaltered. For the recharge, consideration is given to the FEFLOW model with recharge values calibrated with the HELP model because recharge and hydraulic conductivity values are generally highly correlated and

ESDD
6, 1339–1394, 2015

different sets of recharge-conductivity values can provide similar calibration results. For each cell of the FEFLOW model, the steady-state flow model uses the mean annual groundwater recharge estimated from the calibrated HELP model for the 1971–2001 period, to adjust hydraulic conductivities (horizontal and vertical) for each FEFLOW model layer. Using a time-averaged recharge value per model cell to represent present-day groundwater recharge conditions is justified by the facts that: (1) no significant changing trend is observed in water table elevation at available long-term monitoring well hydrographs over the Island (Rivard et al., 2009); and (2) measured head data were collected over a considerable period of time (> 40 years).

A comparison of the observed and predicted hydraulic heads shows that the slope of the best-fit line is very close to 1.0 (1 : 1 line) and the coefficient of correlation (r) of 0.95 expresses a fair amount of scatter (Fig. 6a). The estimated error is also below 8 % over the range of heads observed within the Island (RMS error of 8.51 m for a hydraulic head range of approximately 110 m). This is consistent with the fact that the observed head data were measured over several ten of years and likely reflect transient intra and inter-annual head variations.

Table 4 summarizes model parameters used for the head calibration. The calibrated horizontal hydraulic conductivities show the same general trends as field-based values. The hydraulic conductivity anisotropy ratio for each model layer was based on the field hydraulic conductivity profiles and laboratory fracture analysis of Francis (1989). Generally, both the top of the high-flow system (layers 1 and 2) and the deeper part of the low-flow system (layers 7 and 8) has a low anisotropy ratio. The former is due to the highly fractured conditions of the sandstone, and the latter, to the absence of fractures. The lower end of the high-flow system (layers 3 and 4) and the shallowest part of the low-flow system (layers 3 and 6) has the highest anisotropy ratios due to the presence of a few scattered fractures.

ESDD
6, 1339–1394, 2015

3.4.2 Baseflow-recession calibration

Once an acceptable match was obtained under steady-state conditions, the resulting model was used to simulate transient baseflow under recession conditions for the main rivers (Morell, Wilmot, Winter; Fig. 6b). With this procedure, groundwater recharge for the model is set to zero and daily discharge through the river nodes are compared to specific baseflow-recession events extracted from streamflow records. Baseflow-recession events for PEI occur generally at the end of summer during long periods of time without rainfall, when rivers are solely sustained by groundwater. The rate of decline of baseflow-recession curves is sensitive to a specific yield value, which controls the amount of water that can drain from the aquifer to the connected rivers (Mendoza et al., 2003; Sánchez-Murillo et al., 2015). A lower specific yield value is thus associated to a faster drainage of the aquifer. This dynamics is linked with groundwater and nitrate residence time that may have an important impact on the capabilities of the numerical model to predict meaningful groundwater nitrate concentration.

The modelling of baseflow-recession events for the Wilmot River shows the best adjustment for a specific yield value of 1 %, which is attributed to the fractures in the sandstone aquifer (Fig. 6b). Note that recession curves are mostly sensitive to the high-flow layers, and specific yield values for underlying layers were progressively lowered to represent the decreasing number of fractures with depth (Table 4).

3.4.3 Nitrate concentrations calibration

The mass of nitrogen leaching to the aquifer was applied under transient conditions and adjusted to match nitrate concentrations measured in more than 17 000 domestic wells for the 2000–2005 period. In PEI, intensive agriculture began around 1965 with the introduction of chemical fertilizers and steadily increased since that time. The model of Paradis et al. (2006, 2007) for the Wilmot River watershed has illustrated the considerable time lag between increased leaching of nitrogen and the build up of groundwater nitrate concentrations corresponding to this increased input. This lag time is due to

ESDD
6, 1339–1394, 2015

both the large capability of the PEI aquifer system to accumulate nitrate because of the large porosity of the sandstone, and the typically long residence time of groundwater from its recharge to its outflow in rivers. The maximum residence time of the high-flow and the shallow low-flow systems before discharge to the Wilmot River watershed was up to 20 and 10 000 years, respectively. It can be assumed that a similar situation exists over the entire PEI aquifer system and that groundwater nitrate concentration is presently not in steady state equilibrium with the nitrate loadings that have historically prevailed in watersheds throughout PEI.

Consequently the numerical model needs to be run under transient conditions with the historical record of nitrate flux reaching the aquifer to ensure realistic predictions of groundwater nitrate concentrations. Because RSN values were only estimated based on the 5 census years (1981, 1986, 1991, 1996, 2001), no RSN estimate is available prior to 1981. Thus, for the onset of intensive agriculture in PEI from 1965 to 1981, an average mass representing the nitrate load for this period was adjusted to match observed present-day nitrate concentrations. For modelling purposes, it was assumed that all available RSN is transformed into nitrate and transferred to the aquifer within the year of application, as demonstrated by Ballard et al. (2009). Moreover, the estimates of mass of nitrate leaching to the aquifer based on the last 5 census years were not modified during the calibration process. As previously demonstrated using nitrate stable isotopes by Savard et al. (2007), no significant denitrification occurs in both the unsaturated and the saturated zones in PEI. Therefore, only advective-dispersive transport was considered in this study.

Groundwater flow and nitrate transport were then run under steady-state and transient conditions, respectively, using hydraulic parameters summarized in Table 4. Total porosity was based on average laboratory values (Francis, 1989), whereas the effective diffusion coefficient, and longitudinal and transverse dispersivities used for the transport simulations were $1 \times 10^{-9}\,m^2\,s^{-1}$, 5 and 0.5 m, respectively, considering typical groundwater flow path lengths (Gelhar et al., 1992). As depicted in Fig. 6c, the average nitrate concentration measured in wells generally agrees with the simulated concentra-

ESDD
6, 1339–1394, 2015

D. Paradis et al.

tion for the SLC polygons for which RSN values are available. Simulated concentration is the average nitrate concentration for the first four layers representing the high-flow system within which most domestic rock aquifer wells used for groundwater sampling are open. However, the simulated concentration slightly underestimates reality (approximately 0.5 $mg L^{-1}$ lower than measurements), as expected from the procedure of nitrogen load application at the model surface previously discussed.

4 Results of modelling

On the basis of the previous calibration results, it is assumed that the FEFLOW model provides a good representation of groundwater flow conditions and nitrate transport in the PEI aquifer system as well as of present-day nitrate concentration in drinking water. For the purposes of this study, and knowing the uncertainty about groundwater recharge, hydraulic conductivity, specific yield, porosity and nitrate loadings, consideration will thus be given to the relative changes of future scenarios with respect to the calibrated FEFLOW model (see next sections).

4.1 Future climate scenarios

The generated future climate scenarios show considerable warming from both GCMs (Table 5), although CGCM2 projected much greater warming than HadCM3 for the Charlottetown weather station (Fig. 1). Also, minimum temperature increases more markedly than maximum temperature, and warming under scenario A2 is more noticeable than under B2, as expected from higher CO_2 emissions. While warming is expected throughout the entire year (July and January) for all scenarios, changes in precipitation appear uncertain, with total monthly precipitation and number of days with precipitation increasing or decreasing according to a specific scenario or season. Indeed, CGCM2 projects a slight decrease in precipitation for January with the opposite for HadCM3, even though the number of days with precipitation decreases in January

ESDD
6, 1339–1394, 2015

for all scenarios. However, the projected July precipitation for 2040–2069 shows an increase or no change relative to the 1971–2000 averages for all four scenarios.

Scenario CGCM2-A2 shows a decrease in precipitation intensity during July (summer), as the number of days with precipitation increases and total precipitation remains unchanged. This can thus have an impact on surface runoff because a decrease in precipitation intensity results in less excess water to runoff during rainfall events. The scenario HadCM3-A2 shows on the contrary an increase in precipitation intensity for July. For January (winter), the surface runoff dynamics is more complex as snowpack thawing and form of precipitation (snow vs. rain) should be taken into account as previously done with the HELP model.

4.2 Hydrologic cycle components and groundwater recharge

Simulation results for the historic period (1970–2001) show that almost 50 % (583 mm) of the annual precipitation is returned to the atmosphere by evapotranspiration (Table 6). Another 19 % (221 mm) is flowing to the rivers by surface runoff, and 31 % (369 mm) infiltrates the soil down to the sandstone aquifer as groundwater recharge. Moreover, groundwater recharge over the Island varies from 0 mm yr^{-1} in wetland areas, to 704 mm yr^{-1} over coarse sand soil (Fig. 7). The standard-deviation for groundwater recharge values is 50 mm/yr, in accordance with the homogeneity observed at the Island scale for climate as well as for the soil and geology.

For the 2040–2069 period, evapotranspiration values increase for all climate scenarios, as expected from the increase in temperature for the same period (Table 6). However, the variation in evapotranspiration is less marked than the variation in temperature. For surface runoff, values are predicted to be unchanged or decreased, with large variations ranging from 0 to 66 mm (Table 6). Those variations between scenarios are mainly related to the total precipitation available, evapotranspiration, decrease in precipitation intensity and snowpack dynamics as previously discussed. Total precipitation and groundwater recharge variations between scenarios follow similar patterns with increased values for the A2 scenarios (CGCM2 and HadCM3) and decreased

ESDD
6, 1339–1394, 2015

values for the B2 scenarios with respect to the historic period (Table 6). In general, a decrease in groundwater recharge is expected for the 2040–2069 period; only the CGCM2-B2 scenario leads to an increase in recharge. On average, for the four scenarios, recharge is expected to decrease by only 4 % (15 mm) relative to the historic period.

4.3 Residual soil nitrogen

The components of the nitrogen balance were averaged over the 23 SLC polygons in PEI (Table 7). The total amount of nitrogen input from fertilizer, manure, leguminous crops and atmospheric deposition is 102.3 kg N ha^{-1}. The outputs consist in nitrogen removed by cropping and gaseous losses, which total 71.5 kg N ha^{-1}. The province-wide average RSN is therefore 30.8 kg N ha^{-1}. The spatial variability of RSN ranges from less than 25 to approximately 40 kg N ha^{-1} according to the local agricultural management practices (Fig. 8a).

With the agricultural adaptation scenario, nitrogen inputs from fertilizer were predicted to increase by 8.4 kg N ha^{-1} relative to historical inputs (Table 7). The other inputs from manure, fixation and deposition remained relatively constant. Nitrogen removal by crop uptake increases by 3.1 kg N ha^{-1}, and consequently residual soil nitrogen at the end of the growing season increases significantly from 30.8 kg N ha^{-1} under historical management, to 35.7 kg N ha^{-1} with the simulated adaptation scenario (16 % increase). The spatial variability of RSN under the adaptation scenario ranges from 28.3 to 46.1 kg N ha^{-1} (Fig. 8b). The increase in RSN relative to historical data ranges from 10 to 23 %.

4.4 Nitrate concentration evolution simulations

To assess the potential impact of climate change and agriculture adaptation in the future, nine groundwater flow and mass transport simulation scenarios were defined:

ESDD
6, 1339–1394, 2015

- Scenario 1 (Fig. 9b): this is the baseline scenario, which uses the mean historical groundwater recharge (steady-state flow) and the present-day agricultural practices (steady-state transport with RSN values from the 2001 census) from 2001 until 2069. This scenario is used to assess when aquifer concentrations are reaching steady-state conditions using present-day nitrate loadings (equilibrium between nitrogen input and output from the aquifer).
- Scenarios 2 to 5 (Fig. 10a–d): these scenarios use the present-day agricultural practices (steady-state transport) in the SLC polygons but their groundwater recharge is based on the values obtained from the four climate scenarios (transient flow). The mass of nitrate applied over the watershed is kept constant for the 23 SLC polygons from 2001 until 2069. This mass represents the mean RSN value from the 5 past censuses (1981, 1986, 1991, 1996 and 2001). These scenarios aim at assessing the impact of climate change alone without agricultural adaptation and nitrate concentrations equilibrium.
- Scenarios 6 to 9 (Fig. 11a–d): these simulations use the RSN values modelled for the 2040–2069 period (transient transport) with the four climate scenarios along with the groundwater recharge based on the values obtained from these climate scenarios (transient flow). These scenarios are used to assess the impact of agricultural adaptation alone, and combine the impact of nitrate concentrations equilibrium, climate changes and agricultural adaptation.

Given that the doubling of CO_2 in the atmosphere is to be reached in 2050, the future climate scenarios for temperatures and precipitation are available for the 2040–2069 period only. For the modelling purposes of this study, the gap between the last year of the calibration period (2001) and the beginning of the scenarios (2040) was then filled with gradual changes in groundwater recharge and RSN values to provide meaningful nitrate concentrations in the future. A linear interpolation between values established for 2001 and 2040 was thus applied.

ESDD
6, 1339–1394, 2015

Figure 9a presents map of the average nitrate concentration per watershed for the present-day (2001) conditions obtained from the calibrated FEFLOW model. For comparison purposes, modelled groundwater nitrate concentrations were divided into four classes: background ($< 1\,\mathrm{mg\,L^{-1}}$), low ($1–3\,\mathrm{mg\,L^{-1}}$), medium ($3–5\,\mathrm{mg\,L^{-1}}$) and high ($> 5\,\mathrm{mg\,L^{-1}}$). These classes are used to emphasize that the model is more indicative of relative spatio-temporal changes in groundwater nitrate concentrations rather than absolute concentration values, as expected from the process of nitrogen load application at the surface of the model previously discussed. This map shows that the most impacted watersheds are in the center of the Island where most agricultural activities are taking place. Histograms of the number of watersheds in each class reveal that 42 % of the watersheds are in the medium (17) or high (4) nitrate concentration classes (Fig. 9a; Table S1 in the Supplement). This observation reflects the critical situation PEI is in regarding groundwater quality related to nitrate contamination.

Compared to the present-day situation (Fig. 9a), the average increases in nitrate concentration for the 2050 baseline scenario (scenario 1; Fig. 9b) is 11 % for the Island (Table S1). This increase reflects steady-state in groundwater concentration due to gradual loading of nitrate using present-day concentration. Note that for the sake of simplification results are presented for 2050, the year when atmospheric CO_2 is predicted to have doubled relative to 1990's atmospheric level. Under the 2050 baseline scenario, the average nitrate content of several watersheds moves in a higher concentration class, 50 % to the medium (17) and high (8) classes. The 2050 results show no more watershed at the background level (Fig. 9b; Table S1). Moreover, in the Western part of the Island, several watersheds are predicted to reach the higher class, likely due to the longer residence times, i.e. a longer period before reaching equilibrium.

The average increase in groundwater nitrate concentration over the Island for the four climate scenarios (2–5; Fig. 10a–d) range between 11 and 17 % (Table S1) with respect to the present-day scenario (Fig. 9a). The departures from the baseline scenario (1) suggests that the impact of climate change alone on nitrate concentration for the entire Island is 6 % for CGCM2-A2 and HadCM3-A2, 4 % for HadCM3-B2, and

ESDD
6, 1339–1394, 2015

zero for CGCM2-B2. There is thus also no significant change in nitrate concentration classes and only two watersheds moving from the low to the medium class for all climate scenarios (Fig. 10a–d; Table S1). These simulations indicate that climate change alone (scenarios 2–5) has less impact on future water quality then reaching equilibrium with current nitrate loadings (scenario 1).

The Island average concentration for each climate scenario integrating the various agricultural adaptation scenarios (6 to 9; Fig. 11a–d) indicates a nitrate increase between 25 and 32 % (Table S1) relative to the present-day simulation (Fig. 9a). The scenarios with CGCM2-A2 (scenario 6, Fig. 11a) and HadCM3-A2 (scenario 8, Fig. 11c) predict the highest impacts with 64 % of the watersheds in the medium (17) or the high (8) class, while the scenario with CGCM2-B2 (scenario 7, Fig. 11b) has the lowest impact (58 % in medium or high class). The center of the Island is the region the more strongly affected by high nitrate concentrations, as expected from the intensification of agricultural activities for the 2049–2069 period (Fig. 8b). Moreover, the comparison of the scenarios that consider agricultural adaptation (scenarios 6 to 9) with the baseline scenario (scenario 1) indicates that changes in agricultural practices would have an impact on the increase of average nitrate concentration between 14 and 21 % (Table S1). Thus agricultural practices changes will potentially have a greater effect on future groundwater nitrate concentration in PEI than climate change alone (0–6 %) or the reach of nitrate concentrations equilibrium in the aquifer system (11 %).

5 Summary

To assess the potential impact of climate change and the foreseen agricultural adaptation on nitrate concentrations in groundwater over the PEI, nine different groundwater flow and mass transport scenarios were considered. Simulations of these scenarios and their results expected for 2050 show that:

ESDD
6, 1339–1394, 2015

- the progressive change of groundwater nitrate concentrations simply due to reaching steady-state conditions related to present-day loading would generate an 11 % increase of concentrations;
- climate change alone would account for an increase of only 0 to 6 %, whereas agricultural adaptation would generate an increase of 14 to 21 %;
- the combined effect of equilibration with loadings, climate and agricultural adaptation would create an increase in nitrate concentration between 25 and 32 % over the PEI aquifer system with climate change alone contributing the least to that increase.

As a consequence, the predicted general trend from 2001 to 2050 is that a significant number of watersheds would belong to the highly impacted group of watersheds having a mean nitrate concentration exceeding 5 mg L^{-1} (N-NO_3) with a recommended maximum concentration limit of 10 mg L^{-1} (N-NO_3) for drinking water. In 2001, 4 watersheds over a total of 50 were in this group compared to 8 predicted for 2050 after reaching steady-state conditions and having undergone some of the climate change, or 9 to 11 after agricultural adaptation is also considered.

Finally, predicting the impact of climate change on groundwater quality in agricultural contexts represents a complex challenge that we have attempted to address using the case study of PEI. In that particular example, the main finding in support to decision making for sustainable development is that predicted climatic conditions combined with agricultural practices adapted to these conditions may be expected to generate significant degradation of water quality that would require modifying water servicing infrastructures, and develop better agricultural management practices to reduce nitrate loadings to the aquifer system (e.g. Zebarth et al., 2015; Somers and Savard, 2015). At a broader scale, we also have made progress in pinpointing key steps to be considered in predictive modelling, particularly in highlighting the need to produce sound and realistic scenarios of region-specific agricultural adaptation to climate change while considering the specificity of the hydrogeological processes taking place.

ESDD
6, 1339–1394, 2015

The Supplement related to this article is available online at doi:10.5194/esdd-6-1339-2015-supplement.

Acknowledgements. This study was funded by Natural Resources Canada (Climate Change Impact and Adaptation), and the Geological Survey of Canada (Groundwater Program). A NSERC Discovery Grant also supported R. Lefebvre. This is an ESS contribution 9999.

References

Allen, D. M., Mackie, D. C., and Wei, M.: Groundwater and climate change: a sensitivity analysis for the Grand Forks aquifer, southern British Columbia, Canada, Hydrogeol. J., 12, 270–290, 2004.

Allen, D. M., Cannon, A. J., Toews, M. W., and Scibek, J.: Variability in simulated recharge using different GCMs, Water Resour. Res., 46, W00F03, doi:10.1029/2009WR008932, 2010.

Ballard, J.-M., Paradis, D., Lefebvre, R., and Savard, M. M.: Numerical modeling of the dynamics of multisource nitrate generation and transfer, PEI, GeoHalifax '09, Paper 210, 62th Canadian Geotechnical Conference and 10th Joint CGS/IAH Conference, 20–24 September 2009, Halifax, Canada, 1507–1514, 2009.

Beigi, E. and Tsai, F. T.-C.: Comparative study of climate-change scenarios on groundwater recharge, southwestern Mississippi and southeastern Louisiana, USA, Hydrogeol. J., 23, 789–806, 2015.

Bootsma, A., Gameda, S., McKenney, D. W.: Adaptation of agricultural production to climate change in Atlantic Canada, Final report for Climate Change Action Fund Project A214, Agriculture and Agri-Food Canada, Eastern Cereal and Oilseed Research Centre, Ottawa, Canada, 30 pp., 2001.

Burns, D. A., Klaus, J., and McHale, M. R.: Recent climate trends and implications for water resources in the Catskill Mountain region, New York, USA, J. Hydrol., 336, 155–170, 2007.

Burton, D. L. and Beauchamp, E. G.: Nitrogen losses from swine housings, Agr. Wastes, 15, 59–74, 1986.

Canadian Soil Information System: National Soil Database, Agriculture and Agri-Food Canada, Ottawa, Canada, 2000.

ESDD

6, 1339–1394, 2015

Groundwater nitrate concentration evolution under climate change: Prince Edward Island

D. Paradis et al.

CanImage: Landsat-7 Ortho-Images of Canada, 1/50000, Prince Edward Island, Natural Resources Canada, Centre for Topographic Information, Sherbrooke, Canada, 2001.
Crosbie, R. S., McCallum, J. L., Walker, G. R., and Chiew, F. H. S.: Modelling climate-change impacts on groundwater recharge in the Murray-Darling Basin, Australia, Hydrogeol. J., 18, 1639–1656, 2010.
Croteau, A., Nastev, M., and Lefebvre, R.: Groundwater recharge assessment in the Chateauguay River watershed, Can. Water Resour. J., 35, 451–468, 2010.
De Jong, R., Qian, B., and Yang, J. Y.: Modelling nitrogen leaching in Prince Edward Island under Climate change scenarios, Can. J. Soil Sci., 88, 61–78, 2008.
Diersch, H.-J. G.: FEFLOW: Finite Element Subsurface Flow and Transport Simulation System-Reference Manual, v.6.0., WASY GmbH Software, Berlin, 277 pp., 2010.
Drury, C. F., Yang, J. Y., De Jong, R., Yang, X. M., Huffman, E., Kirkwood, V., and Reid, K.: Residual soil nitrogen indicator for Canada, Can. J. Soil Sci., 87, 166–177, 2007.
Ducharne, A., Baubion, C., Beaudoin, N., Benoit, M., Billen, G., Brisson, N., Garnier, J., Kieken, H., Lebonvallet, S., Ledoux, E., Mary, B., Mignolet, C., Poux, X., Sauboua, E., Schott, C., Theìry, S., and Viennot, P.: Long term prospective of the Seine River system: confronting climatic and direct anthropogenic changes, Sci. Total Environ., 375, 292–311, 2007.
Flato, G. M. and Boer, G. J.: Warming asymmetry in climate change simulations, Geophys. Res. Lett., 28, 195–198, 2001.
Francis, R. M.: Hydrogeology of the Winter River Basin, Prince Edward Island, Department of the Environment, Water Resources Branch, Prince Edward Island, 117 pp., 1989.
Furey, P. R. and Gupta, V. K.: A physically based filter for separating base flow from streamflow time series, Water Resour. Res., 37, 2709–2722, 2001.
Gelhar, L. W., Welty, C., and Rehfeldt, K. R.: A critical review of data on field-scale dispersion in aquifers, Water Resour. Res., 28, 1955–1974, 1992.
Ghiglieri, G., Barbieri, G., Vernier, A., Carletti, A., Demurtas, N., Pinna, R., and Pittalis, D.: Potential risks of nitrate pollution in aquifers from agricultural practices in the Nurra region, northwestern Sardinia, Italy, J. Hydrol., 379, 339–350, 2010.
Gleick, P. H.: Methods for evaluating the regional hydrologic impacts of global climatic changes, J. Hydrol., 88, 91–116, 1986.
Gordon, C., Cooper, C., Senior, C. A., Banks, H., Gregory, J. M., Johns, T. C., Mitchell, J. F. B., and Wood, R. A.: The simulation of SST, sea ice extents and ocean heat transports in a

ESDD
6, 1339–1394, 2015

version of the Hadley Centre coupled model without flux adjustments, Clim. Dynam., 16, 147–168, 2000.
Green, T. R., Taniguchi, M., and Kooi, H.: Potential impacts of climate change and human activity on subsurface water resources, Vadose Zone J., 6, 531–532, 2007a.
Green, T. R., Bates, B. C., Charles, S. P., and Fleming, P. M.: Physically based simulation of potential effects of carbon dioxide altered climates on groundwater recharge, Vadose Zone J., 6, 597–609, 2007b.
Hagg, W., Braun, L. N., Huhn, M., and Nesgaard, T. I.: Modelling of hydrological response to climate change in glacierized Central Asia catchments, J. Hydrol., 332, 40–53, 2007.
Hayhoe, H. N.: Improvements of stochastic weather data generators for diverse climates, Clim. Res., 14, 75–87, 2000.
Health Canada: Summary of guidelines for Canadian drinking water quality, Prepared by the Federal–Provincial-Territorial Committee on Drinking Water of the Federal–Provincial-Territorial Committee on Health and the Environment, available at: http://www.hc-sc.gc.ca/ewh-semt/pubs/water-eau/sum_guide-res_recom/index-eng.php (last access: August 2015), 2014.
Hengeveld, H. G.: Projections for Canada's Climate Future: A Discussion of Recent Simulations with the Canadian Global Climate Model, Science Assessment and Integration Branch, Meteorological Service of Canada, Downsview, Ontario, Canada, 27 pp., 2000.
Holman, I. P., Rounsevell, M. D. A., Shackley, S., Harrison, P. A., Nicholls, R. J., Berry, P. M., and Audsley, E.: A regional, multi-sectoral and integrated assessment of the impacts of climate and socio-economic change in the UK: Part 1 Methodology, Climatic Change, 71, 9–41, 2005a.
Holman, I. P., Nicholls, R. J., Berry, P. M., Harrison, P. A., Audsley, E., Shackley, S., and Rounsevell, M. D. A.: A regional, multi-sectoral and integrated assessment of the impacts of climate and socio-economic change in the UK: Part 2 Results, Climatic Change, 71, 43–73, 2005b.
Holman, I. P., Tascone, D., and Hess, T. M.: A comparison of stochastic and deterministic downscaling methods for modelling potential groundwater recharge under climate change in East Anglia, UK: implications for groundwater resource management, Hydrogeol. J., 17, 1629–1641, 2009.

ESDD
6, 1339–1394, 2015
Groundwater nitrate concentration evolution under climate change: Prince Edward Island
D. Paradis et al.

Hsu, K.-C., Wang, C.-H., Cheu, K.-C., Chen, C.-T., and Ma, K.-W.: Climate-induced hydrological impacts on the groundwater system of the Pingtung Plain, Taiwan, Hydrogeol. J., 15, 903–913, 2007.

Huffman, T., Ogston, R., Fisette, T., Daneshfar, B., Gasser, P. Y., White, L., Maloley, M., and Chenier, R.: Canadian agricultural land-use and land management data for Kyoto reporting, Can. J. Soil Sci., 86, 431–439, 2006.

IPCC – International Panel on Climate Change: Climate Change 2001 – Working Group I: The Scientific Basis, available at: http://www.grida.no/climate/ipcc_tar/wg1/index.htm (last access: August 2015), 2001.

Jackson, B. M., Wheater, H. S., Wade, A. J., Butterfield, D., Mathias, S. A., Ireson, A. M., Butler, A. P., McIntyre, N. R., and Whitehead, P. G.: Catchment-scale modelling of flow and nutrient transport in the Chalk unsaturated zone, Ecol. Model., 209, 41–52, 2007.

Jiang, Y. and Somers, G.: Modeling effects of nitrate from non-point sources on groundwater quality in an agricultural watershed in Prince Edward Island, Canada, Hydrogeol. J., 17, 707–724, 2009.

Jyrkama, M. I. and Sykes, J. F.: The impact of climate change on spatially varying groundwater recharge in the grand river watershed (Ontario), J. Hydrol., 338, 237–250, 2007.

Jyrkama, M. I., Sykes, J. F., and Normani, S. D.: Recharge estimation for transient ground water modelling, Ground Water, 40, 638–648, 2002.

McCallum, J. L., Crosbie, R. S., Walker, G. R., and Dawes, W. R.: Impacts of climate change on groundwater in Australia: a sensitivity analysis of recharge, Hydrogeol. J., 18, 1625–1638, 2010.

McGinn, S. M. and Shepherd, A.: Impact of climate change scenarios on the agroclimate of the Canadian prairies, Can. J. Soil Sci., 83, 623–630, 2003.

Mendoza, G. F., Steenhuis, T. S., Walter, M. T., and Parlange, J. Y.: Estimating basin-wide hydraulic parameters of a semi-arid mountainous watershed by recession-flow analysis, J. Hydrol., 279, 57–69, doi:10.1016/S0022-1694(03)00174-4, 2003.

Monfet, J.: Eìvaluation du coefficient de ruissellement à l'aide de la meìthode SCS modifieìe, Service de l'hydromeìtrie, Ministère des Richesses Naturelles, Publication HP-51, Gouvernement du Queìbec, Queìbec, 35 pp. 1979.

Mutch, J.: The hydrologic cycle and water movement, Nitrate-agricultural sources and fate in the environment-perspectives and direction. Proceedings of the workshop, Eastern Canada Soil and Water Conservation Centre, Charlottetown, Canada,3–7, 1998.

Nakicenovic, N. and Swart, R.: Special Report on Emissions Scenarios – A Special Report of Working Group III of the Intergovernmental Panel on Climate Change, Cambridge University Press, Cambridge, UK, 612 pp., 2000.

Okkonen, J., Jyrkama, M., and Kløve, B.: A conceptual approach for assessing the impact of climate change on groundwater and related surface waters in cold regions (Finland), Hydrogeol. J., 18, 429–439, 2010.

Olesen, J. E. and Bindi, M.: Consequences of climate change for European agricultural productivity, land use and policy, Eur. J. Agron., 16, 239–262, 2002.

Ontario Ministry of Agriculture and Food: Soil Fertility Handbook, Publication 611, Ontario Ministry of Agriculture and Food, Ottawa, Canada, 2003.

Paradis, D., Ballard, J.-M., Savard, M. M., Lefebvre, R., Jiang, Y., Somers, G., Shawna, L., and Rivard, C.: Impact of agricultural activities on nitrate in ground and surface water in the Wilmot Watershed, PEI, Canada, in: Paper 244, Proceedings, 59th Canadian Geotechnical Conference and 7th Joint CGS/IAH Conference, 1–4 October 2006, Vancouver, Canada, 8 pp., 2006.

Paradis, D., Ballard, J.-M., and Lefebvre, R.: Watershed scale numerical modelling of nitrate fate and transport using spatially uniform averaged N-inputs, in: Consequences of Climatic Changes on Contamination of Drinking Water by Nitrates on Prince Edward Island, Report of the Climate Change Action Fund: Impacts and Adaptation (A881/A843),edited by: Savard, M. M. and Somers, G., Natural Resources Canada, Ottawa, Canada, 49–62, 2007.

Prest, V. K.: Surficial Deposits of Prince Edward Island, Geological Survey of Canada, A-Series Map 1366A, Geological Survey of Canada, Ottawa, Canada, 1973.

Qian, B. D., Gameda, S., Hayhoe, H., De Jong, R., and Bootsma, A.: Comparison of LARS-WG and AAFC-WG stochastic weather generators for diverse Canadian climates, Clim. Res., 26, 175–191, 2004.

Qiang, B. and De Jong, R.: Modelling four Climate change scenarios for Prince Edward Island, in: Consequences of Climatic Changes on Contamination of Drinking Water by Nitrates on Prince Edward Island, Report of the Climate Change Action Fund: Impacts and Adaptation (A881/A843),edited by: Savard, M. M. and Somers, G., Natural Resources Canada, Ottawa, Canada, 63–71, 2007.

Risser, D. W., Gburek, W. J., and Folmar, G. J.: Comparison of methods for estimating groundwater recharge and base flow at a small watershed underlain by fractured bedrock in the

ESDD
6, 1339–1394, 2015

eastern United States, USGS Scientific Investigations Report 2005-5038, USGS, Reston, Virginia, USA, 31 pp., 2005.
Rivard, C., Paradis, D., Paradis, S. J., Bolduc, A., Morin, R. H., Liao, S. L, Pullan, S., Gauthier, M. J., Treìpanier, S., Blackmore, A., Spooner, I., Deblonde, C., Fernandes, R., Castonguay, S., Michaud, Y., Drage, J., and Paniconi, C.: Canadian groundwater inventory: regional hydrogeological characterization of the Annapolis-Cornwallis Valley aquifers, Geological Survey of Canada Bulletin 589, Natural Resources Canada, Ottawa, Canada, 86 pp., 2008.
Rivard, C., Vigneault, H., Piggott, A. R., Larocque, M., and Anctil, F.: Groundwater recharge trends in Canada, Can. J. Earth Sci., 46, 841–854, 2009.
Rivard, C., Lefebvre, R., and Paradis, D.: Regional recharge estimation using multiple methods: an application in the Annapolis Valley, Nova Scotia (Canada), Environ. Earth Sci., 71, 1389–1408, 2014.
Rozell, D. J. and Wong, T.-F.: Effects of climate change on groundwater resources at Shelter Island, New York State, USA, Hydrogeol. J., 18, 657–1665, 2010.
Ruth, M., Bernier, C., Jollands, N., and Golubieswski, N.: Adaptation of urban water supply infrastructure to impacts from climate and socioeconomic changes: the case of Hamilton, New Zealand, Water Resour. Manage., 21, 1013–1045, 2007.
Sánchez-Murillo, R., Brooks, E. S., Elliot, W. J., Gazel, E., and Boll, J.: Baseflow recession analysis in the inland Pacific Northwest of the United States, Hydrogeol. J., 23, 2, 287–303, doi:/10.1007/s10040-014-1191-4, 2015.
Savard, M. M. and Somers, G. (Eds.): Consequences of Climatic Changes on Contamination of Drinking Water by Nitrates on Prince-Edward-Island, Geological Survey of Canada, Agriculture and Agri-Food Canada, PEI Environment, Energy and Forestry, Contribution A881/A843, Report to Natural Resources Canada, Climate Change Action Fund: Impacts and Adaptation, Ottawa, Canada, 20 March 2007.
Savard, M. M., Paradis, D., Somers, G., Liao, S., and van Bochove, E.: Winter nitrification contributes to excess NO_3^- in groundwater of an agricultural region: a dual-isotope study, Water Resour. Res., 43, W06422, doi:10.1029/2006WR005469, 2007.
Savard, M. M., Somers, G., Smirnoff, A., Paradis, D., van Bochove, E., and Liao, S.: Nitrate isotopes unveil distinct seasonal N-sources and the critical role of crop residues in groundwater contamination, J. Hydrol., 381, 134–141, 2010.

Schroeder, P. R., Aziz, N. M., Lloyd, C. M., and Zappi, P. A.: The Hydrologic Evaluation of Landfill Performance (HELP) Model, Engineering documentation for version EPA/600/R-94/168b, Risk reduction Engineering Laboratory Office of Research and Development, USEPA, Cincinnati, Ohio, USA, 116 pp., 1994.
Scibek, J. and Allen, D. M.: Modeled impacts of predicted climate change on recharge and groundwater levels, Water Resour. Res., 42, W11405, doi:10.1029/2005WR004742, 2006.
Serrat-Capdevila, A., Valdés, J. B., González Pérez, J., Baird, K., Mata, L. J., and Maddock III, T.: Modeling climate change impacts and uncertainty on the hydrology of a riparian system: the San Pedro Basin (Arizona/Sonora), J. Hydrol., 347, 48–66, 2007.
Soil Landscapes of Canada Working Group: Soil Landscapes of Canada v3.1, Agriculture and Agri-Food Canada (digital map and database at 1 : 1 million scale), Ottawa, Canada, 2006.
Somers, G.: Distribution and trends for occurrence of nitrate in PEI groundwater, in: Proc. from Nitrate-Agricultural Sources and Fate in the Environment-Perspectives and Direction, Grand Falls, Canada, 1998.
Somers, G. and Mutch, J.: Results of an investigation into the impact of irrigation wells on the availabilty of groundwater in the Baltic area, available at: http://www.gov.pe.ca/photos/original/balticstudy.pdf (last access: August 2015), 1999.
Somers, G. and Savard, M. M.: Shorter fries? An alternative policy to support a reduction of nitrogen contamination from agricultural crop production, Environ. Sci. Policy, 47, 177–185, 2015.
Somers, G. H., Raymond, B., and Uhlman, W.: Prince Edward Island water quality interpretative, Report 99 prepared for Canada-Prince Edward Island Water Annex to Federal/Provincial Framework Agreement for Environmental Cooperation in Atlantic Canada, 67 pp., 1999.
Tóth, J.: A theoretical analysis of groundwater flow in small drainage basins, J. Geophys. Res., 68, 4795–4812, 1963.
USDA – United States Department of Agriculture: Urban hydrology for small watersheds, Soil Conservation Service, Engineering Division, Technical Release 55 (TR-55), Washington, D.C., USA, 1986.
Van de Poll, H. W.: Geology of Prince Edward Island, Prince Edward Island Department of Energy and Forestry, Energy and Minerals Branch, Charlottetown, 66 pp., 1983.
Woldeamlak, S. T., Batelaan, O., and De Smedt, F.: Effects of climate change on the groundwater system in the Grote-Nete catchment, Belgium, Hydrogeol. J., 15, 891–901, 2007.

ESDD
6, 1339–1394, 2015

Groundwater nitrate concentration evolution under climate change: Prince Edward Island

D. Paradis et al.

Yang, J. Y., De Jong, R., Drury, C. F., Huffman, E. C., Kirkwood, V., and Yang, X. M.: Development of a Canadian agricultural nitrogen budget model (CANB v2.0): simulation of the nitrogen indicators and integrated modelling for policy scenarios, Can. J. Soil Sci., 87, 153–165, 2007.

Young, J., Somers, G. H., Raymond, G. B.: Distribution and trends for nitrate in PEI groundwater and surface waters, in: Proc. of National Conference on Agriculture Nutrients and their impact on Rural Water Quality, 29–30 April 2002, Waterloo, Ontario, Agricultural Institute of Canada Foundation, 313–319, 2002.

Yusoff, I., Hiscock, H. D., and Conway, D.: Simulation of the impacts of climate change on groundwater resources in eastern England, Sustainable Groundwater Development, Geol. Soc. Spec. Publ., 193, 325–344, 2002.

Zebarth, B. J., Danielescu, S., Nyiraneza, J., Ryan, M. C., Jiang, Y., Grimmett, M. G., and Burton, D. L.: Controls on nitrate loading and implications for BMPs under intensive potato production systems in Prince Edward Island, Canada, Ground Water Monit. R., 35, 30–42, doi:10.1111/gwmr.12088, 2015.

Zhou, Y., Zwahlen, F., Wang, Y., and Li, Y.: Impact of climate change on irrigation requirements in terms of groundwater resources, Hydrogeol. J., 18, 1571–1582, 2010.

ESDD

6, 1339–1394, 2015

Table 1. Main physiographic and land use characteristics of Prince Edward Island (land use based on a LANDSAT image for 2000).

Physiography	
Area	5660 km^2
Width	3–65 km
Length	225 km
Elevation (a.s.l.)	0–140 m
Land use (%)	
Forest	45
Agriculture	39
Wetland	7
Residential, urban, industrial	5.9
Recreational	0.3
Miscellaneous	2.8

ESDD
6, 1339–1394, 2015

Groundwater nitrate concentration evolution under climate change: Prince Edward Island

D. Paradis et al.

Table 2. Weather for Prince Edward Island (meteorological data for the 1971–2000 period). See Fig. 1 for locations of the weather stations.

Weather characteristic	Station			
	O'Leary	Summerside	Charlottetown	Monticello
Mean annual total precipitation (mm)	1141	1078	1173	1164
Mean annual rain (mm)	860	806	880	903
Mean annual snow (mm)	281	282	311	261
Mean annual temperature (˚C)	5.2	5.6	5.3	5.5
Minimum mean monthly temperature (˚C) (Jan)	−8.6	−7.9	−8.0	−7.4
Maximum mean monthly temperature (˚C) (Jul)	18.5	19.1	18.5	18.4

ESDD
6, 1339–1394, 2015

Table 3. Streamflow characteristics of selected rivers in Prince Edward Island (records are for 1972 to 2005, 1961 to 1995 and 1965 to 1991 for Wilmot, Morell, and Winter rivers, respectively). See Fig. 1 for locations of the rivers.

Streamflow characteristics ($m^3 s^{-1}$)	Watershed (drainage area in km^2)		
	Morell (133)	Wilmot (45)	Winter (38)
Mean annual	2.88	0.92	0.66
Minimum monthly mean (Sep)	1.10	0.44	0.24
Maximum monthly mean (Apr)	6.77	1.89	1.61

ESDD
6, 1339–1394, 2015

Table 4. Field-based and calibrated hydraulic properties of the FEFLOW numerical model for the Prince Edward Island aquifer system.

Model layer (depth in m)	Field K_h ($m\,s^{-1}$)	Numerical model			
		K_h ($m\,s^{-1}$)	K_v/K_h (–)	S_y (%)	n (%)
1 (0–5)	4.5×10^{-4} to 8.1×10^{-5}	3×10^{-4}	0.1	1	17
2 (5–10)		1×10^{-4}	0.1	1	17
3 (10–15)		5×10^{-5}	0.1	1	17
4 (15–30)	1.7×10^{-4} to 8.4×10^{-7}	1×10^{-5}	0.01	1	17
5 (30–80)		1×10^{-5}	0.001	0.1	17
6 (80–180)	n.d.	1×10^{-6}	0.01	0.1	17
7 (180–380)	n.d.	1×10^{-7}	0.1	0.1	17
8 (380–880)	n.d.	1×10^{-8}	1	0.01	17

K_h and K_v: are horizontal and vertical hydraulic conductivity, respectively; S_y: specific yield; n: total porosity.

ESDD
6, 1339–1394, 2015

Table 5. Temperature and precipitation changes for the future period (2040–2069) relative to the historical period (1971–2000) for each selected climate change scenarios at the Charlottetown weather station, Prince Edward Island (Qiang and De Jong, 2007).

Scenario	Temperature change				Precipitation change			
	Monthly mean maximum (°C)		Monthly mean minimum (°C)		Monthly total (%)		Days with precipitation (%)	
	Jan	Jul	Jan	Jul	Jan	Jul	Jan	Jul
CGCM2-A2	1.7	2.5	4.6	3.1	−5.3	0.0	−2.1	5.0
CGCM2-B2	1.1	1.8	4.0	2.2	−8.1	5.0	−3.8	1.8
HadCM3-A2	1.4	1.8	1.7	2.0	4.1	7.7	−5.0	−4.6
HadCM3-B2	1.2	1.4	1.5	1.5	5.1	1.4	−3.0	−1.9

ESDD
6, 1339–1394, 2015

Groundwater nitrate concentration evolution under climate change: Prince Edward Island

D. Paradis et al.

Table 6. Summary of mean annual temperature and hydrologic cycle components (precipitation, evapotranspiration, surface runoff and groundwater recharge) simulated with the HELP model for the historical period (1970–2001) and the four climate scenarios (2040–2069) in Prince Edward Island. Values provided in brackets are the change in mm or °C for the 2040–2069 period compared to historical conditions (1970–2001).

Scenario	Temperature (°C)	Precipitation (mm)	Evapo-transpiration (mm)	Runoff (mm)	Recharge (mm)
Historic	5.3	1173	583	221	369
CGCM2-A2	8.0 (+3.31)	1109 (−64)	618 (+35)	155 (−66)	336 (−33)
CGCM2-B2	7.0 (+2.3)	1223 (+50)	620 (+37)	209 (−12)	394 (+25)
HadCM3-A2	6.7 (+1.4)	1141 (−32)	616 (+33)	202 (−19)	323 (−46)
HadCM3-B2	7.1 (+1.8)	1197 (+24)	615 (+32)	221 (0)	361 (−8)

ESDD
6, 1339–1394, 2015

Groundwater nitrate concentration evolution under climate change: Prince Edward Island

D. Paradis et al.

Table 7. Average components of the nitrogen balance as simulated with historical crop and animal husbandry practices and with an adapted agricultural management scenario (De Jong et al., 2007).

Period	Nitrogen inputs (kg N ha^{-1})						RSN
	Fertilizer	Manure	Fixation	Deposition	Crop	Gas	(kg N ha^{-1})
Historical	52.8	17.4	29.6	2.5	70.3	1.2	30.8
Adapted	61.2	16.8	30.1	2.5	73.2	1.6	35.7

RSN: residual soil nitrogen.

ESDD
6, 1339–1394, 2015

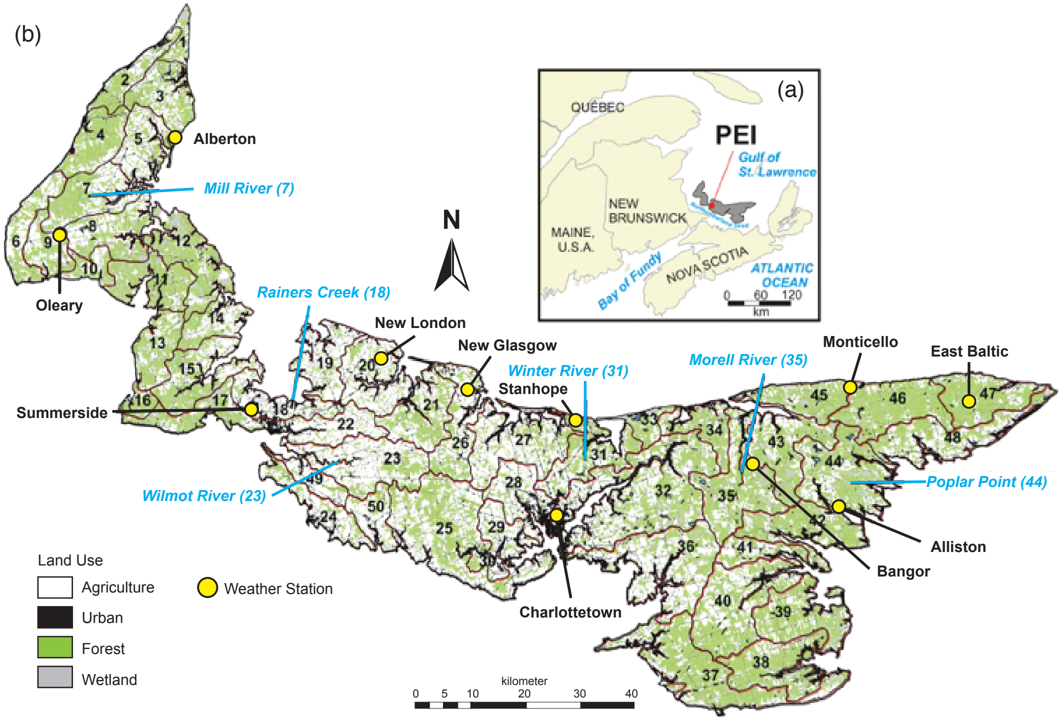

Figure 1. (a) Location of Prince Edward Island (PEI) in eastern Canada. **(b)** Limits of the watersheds (numbered area delineated with brown lines, see names Table S1), with identification of the major rivers (names in blue), along with land use (see legend) and location of the weather stations (names in black).

ESDD
6, 1339–1394, 2015

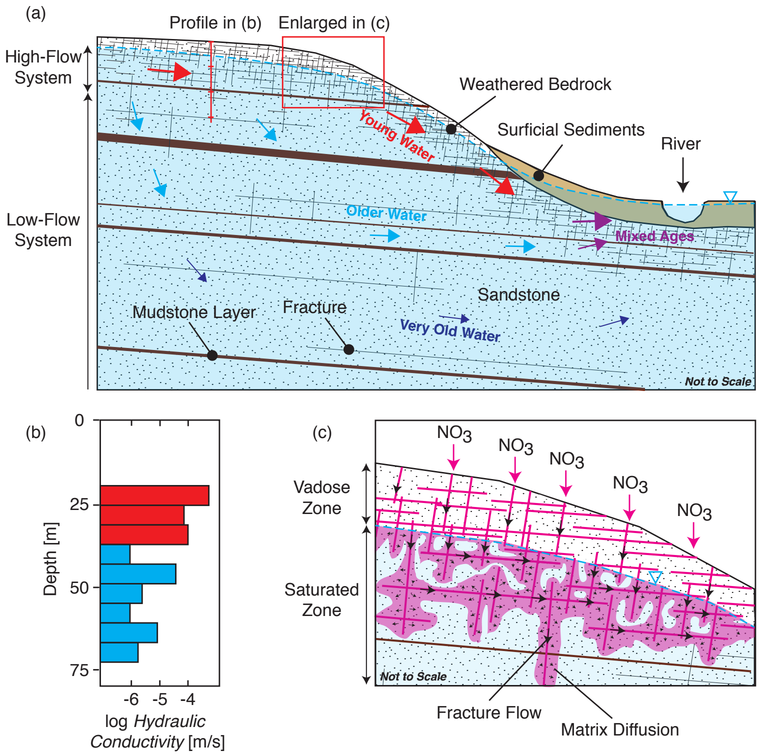

Figure 2. (a) Schematic conceptual model of the groundwater flow system along with **(b)** a typical profile of hydraulic conductivity showing distinct shallow high-flow (red) and deeper low-flow (blue) systems; and **(c)** a conceptualization of nitrate transport in the double-porosity sandstone aquifer with advective fracture flow and matrix diffusion.

ESDD
6, 1339–1394, 2015

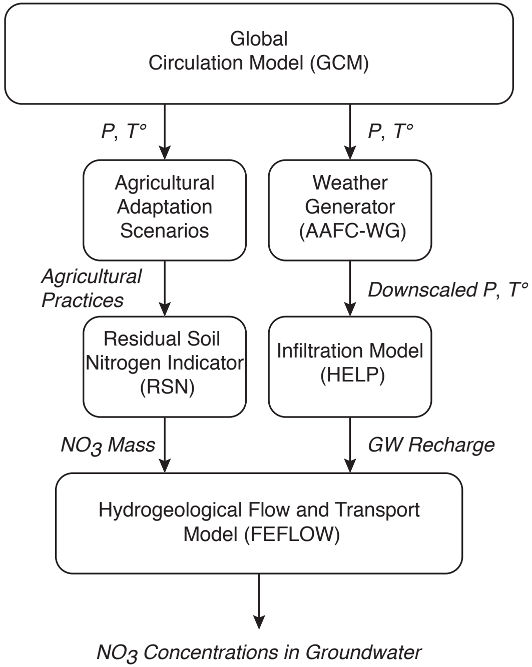

Figure 3. Workflow for the study of the potential impact of climate and agricultural practice changes on future groundwater nitrate concentration in the Prince Edward Island aquifer system.

ESDD
6, 1339–1394, 2015

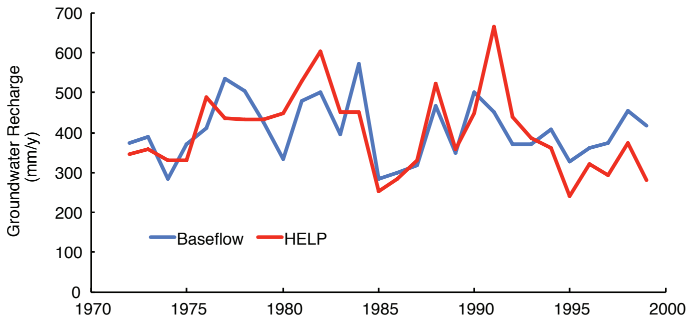

Figure 4. Comparison of the calibrated groundwater recharge values obtained with the HELP model with the baseflow values estimated with the Furey and Gupta (2001) hydrograph separation method for the Wilmot River watershed, for the 1972–1999 period.

ESDD
6, 1339–1394, 2015

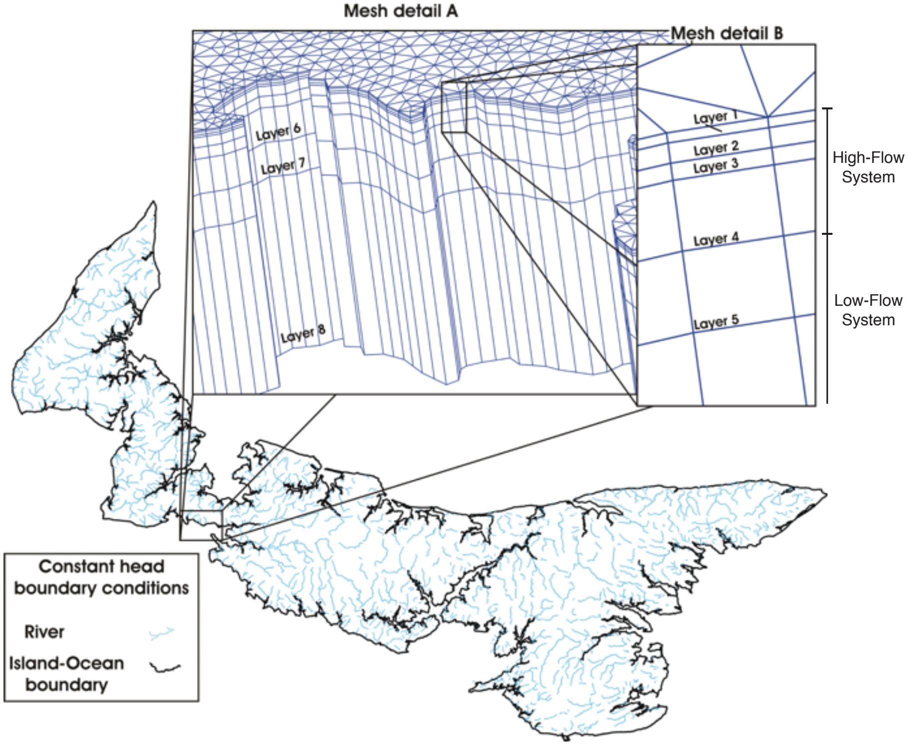

Figure 5. Numerical grid used for the model representing groundwater flow and nitrate transport with the FEFLOW numerical simulator for Prince Edward Island, with grid detail showing the eight layers, the triangular surface elements and boundary conditions. The upper limit of layer 1 was estimated with an adaptive grid thickness simulating fluctuations of the water table elevation.

ESDD
6, 1339–1394, 2015

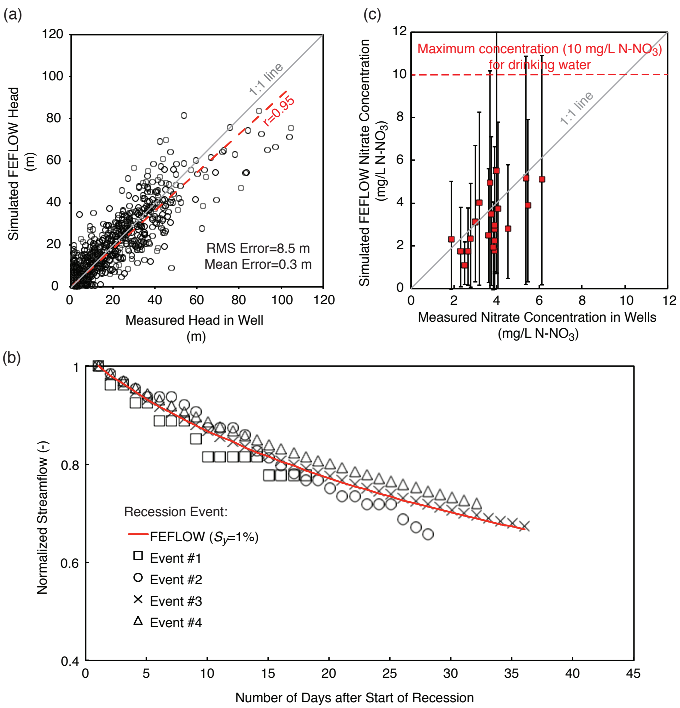

Figure 6. Calibration of the FEFLOW numerical model. **(a)** Comparison of measured heads with simulated heads under steady-state flow conditions, in more than 700 domestic wells distributed over Prince Edward Island; **(b)** example of baseflow calibration of specific yield (S_y) with several streamflow recession events in the Wilmot River under transient conditions with no groundwater recharge applied to the model; and **(c)** model calibration of nitrate transport using the average groundwater nitrate concentration measured in domestic wells for 2002–2005. Each point represents the average nitrate concentration of a single Soil Landscape of Canada (SLC) polygon, whereas the bars span the observed concentration interval from the 25 to the 75 % percentiles.

ESDD
6, 1339–1394, 2015

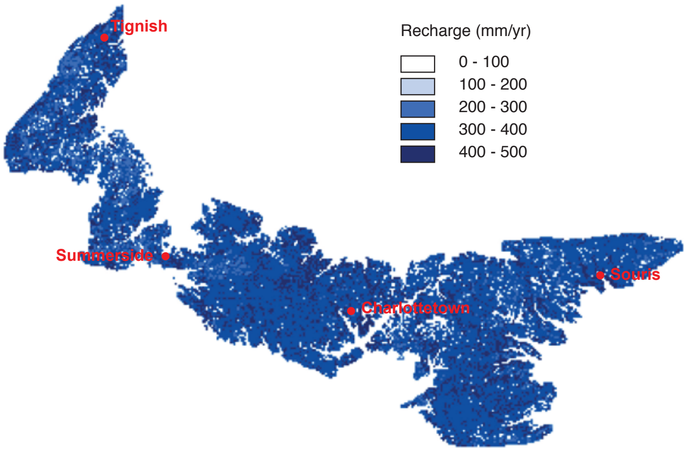

Figure 7. Spatial distribution of groundwater recharge from simulations with the calibrated HELP infiltration model for the historical period (1970–2001). Cell values are averages for the 1970–2001 period. Groundwater recharge is not shown for the 2040–2069 period as no significant changes were obtained from HELP based on climate change scenarios.

ESDD
6, 1339–1394, 2015

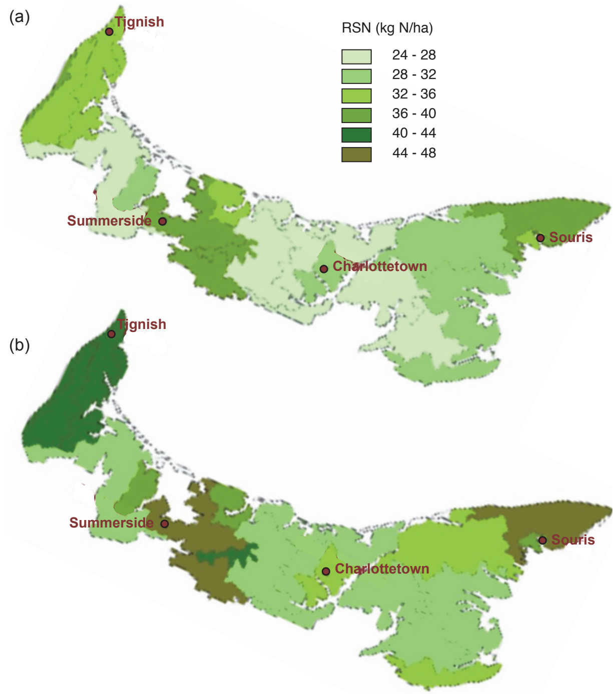

Figure 8. Simulated residual soil nitrogen (RSN) using **(a)** historical management practices and **(b)** the adaptation scenario presented in Table 7 (De Jong et al., 2007). RSN values are for each Soil Landscape of Canada (SLC) polygon.

ESDD
6, 1339–1394, 2015

Groundwater nitrate concentration evolution under climate change: Prince Edward Island

D. Paradis et al.

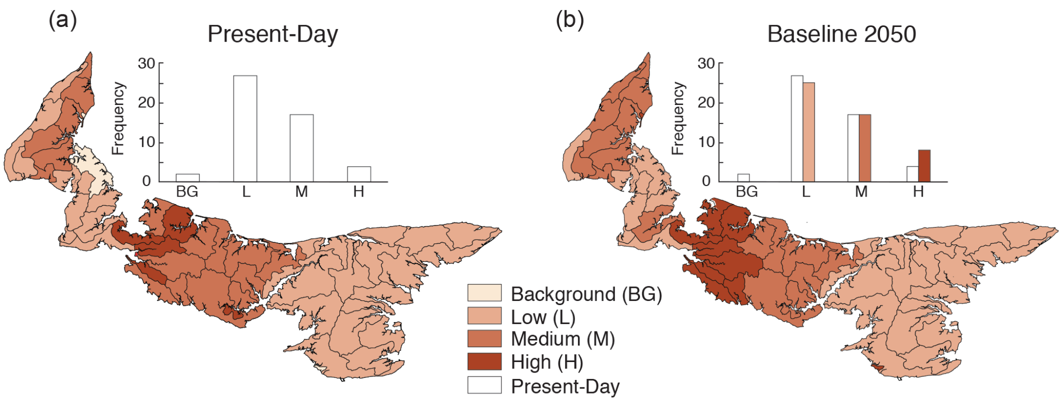

Figure 9. Class distribution of simulated mean nitrate concentration per watershed and histogram of the number of watersheds in each class for: **(a)** present-day (2001); **(b)** 2050 baseline scenario with present-day (2001) nitrate loading and groundwater recharge.

ESDD
6, 1339–1394, 2015

Groundwater nitrate concentration evolution under climate change: Prince Edward Island

D. Paradis et al.

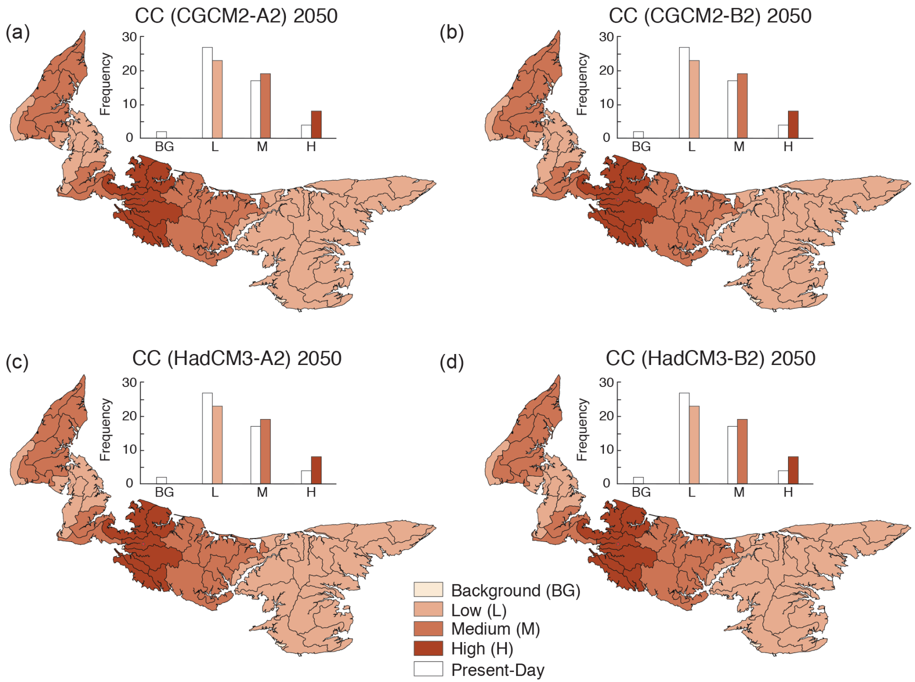

Figure 10. Class distribution of simulated mean nitrate concentration per watershed and histogram of the number of watersheds in each class for the four climate change (CC) scenarios (**a**, **b**, **c** and **d**).

ESDD
6, 1339–1394, 2015

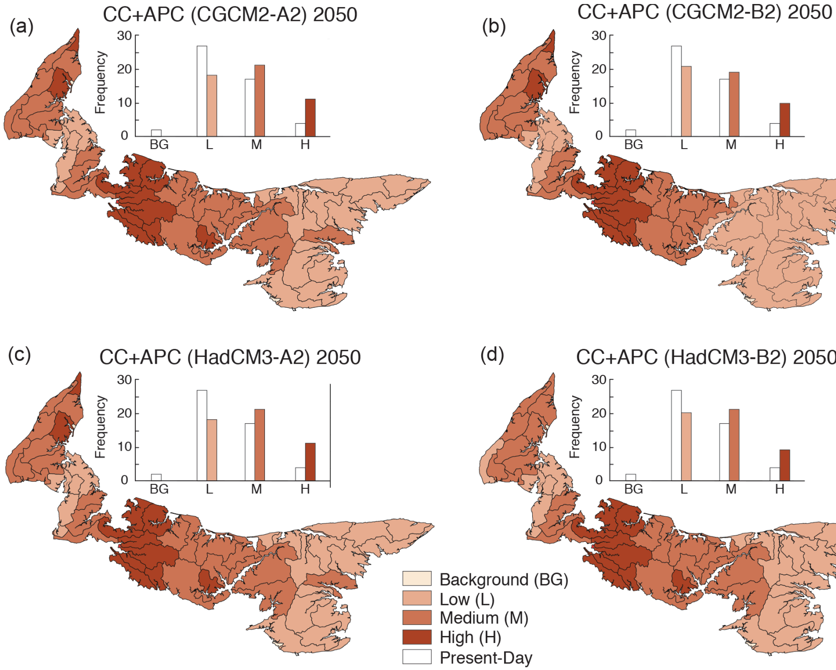

Figure 11. Class distribution of simulated mean nitrate concentration per watershed and histogram of the number of watersheds in each class for the four climate change (CC) scenarios with ensuing agricultural practice adaptation (APC) (**a**, **b**, **c** and **d**).